

# Predictions of tropical rainfall with the ECMWF seasonal and monthly forecast systems

**F. Molteni, F. Vitart, T. Stockdale, L. Ferranti, M. Balmaseda**

*European Centre for Medium-Range Weather Forecasts  
Reading, U.K.*

## **1. Introduction**

Despite recent advances in numerical weather and climate forecasting systems, the prediction of monsoon rainfall over large parts of the tropical land masses remains a challenging problem, which still appears to be far from a satisfactory solution. Traditionally, a clear separation existed between the methodologies used for short-range weather forecasts and for seasonal-scale forecasts of monsoon rainfall, the former mainly relying on deterministic numerical forecasts, the latter originating either from statistical schemes or from ensemble integrations of coupled ocean-atmosphere models. Whereas progress on the short-range time scale has been recently achieved by a combination of better, higher-resolution numerical models, improved data assimilation systems and the extension of ensemble techniques, progress on the seasonal scale has been somewhat episodic and difficult to ascertain. For example, with regard to Indian monsoon rainfall, concern about the ability of currently available systems to produce effective predictions has been expressed by Gadgil et al. (2005); and Xavier and Goswami (2007) claimed that statistical models of rainfall evolution over a 2-to-4 week time scale may provide more useful information than seasonal-mean estimates from coupled GCMs.

In discussing such a complex topic, it is useful to distinguish between a number of distinct issues:

- 1) Are forecasts of seasonal-mean rainfall useful to the users' community, or should focus be shifted to the weekly-to-monthly time-scale?
- 2) In the hypothesis that seasonal-mean predictions do have a value, what is the intrinsic limit of predictability for such averages, as a function of time and location?
- 3) Is the actual predictive skill obtained with coupled dynamical models close to the estimated predictability limit, and if not, are models failing to capture the large-scale anomalies in the monsoon circulation, or are errors in precipitation arising from incorrect representation of local effects (i.e. dependence of convection on land-surface properties, interaction with steep topography, etc.)?
- 4) When considering the weekly-to-monthly scale, do ensembles of high-resolution numerical integrations provide useful probabilistic skill induced by initial conditions, or are they outperformed by statistical schemes?

This paper (partially) addresses the last three questions, under the assumption that forecasts on both seasonal and monthly time scales have potential value for societal applications (see Webster et al., 2006). Specifically, we present results from integrations performed with the latest version of the seasonal and monthly systems of ECMWF, focussing on rainfall over India, west and east Africa. Starting with the seasonal scale, the next section briefly described the so-called ECMWF Seasonal Forecast System-3, the set of hindcast ensembles used for its calibration and assessment, and the forecasts products which provide information about rainfall anomalies. In section 3, potential and actual predictive skill for seasonal mean rainfall over several regions will be compared. A simple filtering technique based on EOF analysis will be discussed in section 4,

showing how it can be used to increase predictive skill over the tropical continents. In section 5, we'll show how forecasts obtained with the latest version of the ECMWF monthly forecasting system (recently merged with the Variable-Resolution Ensemble Prediction System, VAREPS) can provide valuable information on pentad to monthly time scale at the beginning of the Indian monsoon season. Concluding remarks are presented in section 6.

## **2. Seasonal forecasting at ECMWF: system configuration and products**

### **2.1. Configuration of ECMWF Seasonal Forecast System 3**

ECMWF has been running a seasonal forecast system since 1997, and in March 2007 a new forecast system, known as System 3 (S3) was introduced (Anderson et al. 2007). A system consists of the atmospheric and oceanic components of the coupled model as well as the data assimilation scheme to create initial conditions for the ocean, the coupling interface linking the two components and the strategy for ensemble generation. As in previous ECMWF systems, no dynamic sea-ice model is used; the initial conditions are based on the observed sea-ice limit but thereafter the sea-ice evolves according to damped persistence.

The atmospheric model for S3 is cycle 31r1 (Cy31r1) of the ECMWF Integrated Forecasting System (IFS). Compared to the previous seasonal forecast system (S2), the horizontal resolution has been increased from T<sub>L</sub>95 to T<sub>L</sub>159 (with the corresponding grid mesh reduced from 1.875° to 1.125°), and the vertical resolution is increased from 40 levels to 62 levels, extending up to ~5 hPa. The ocean component of the system is the Hamburg Ocean Primitive Equation model (HOPE). Major changes have taken place in the ocean analysis system for S3 (see below), though the HOPE ocean model is little changed from the version used in S2.

The real-time ensemble set consists of 41 members in S3, and the calibration set consists of 11 members spanning the 25-year period 1981–2005, so creating a calibration probability distribution function of 275 members. Each of these ensembles has a start date on the first of the month. As in S2, the ocean initial conditions in S3 are provided not from a single ocean analysis but from a 5-member ensemble of ocean analyses, created by adding perturbations to the wind forcing used in the analysis. The atmospheric initial conditions, including land conditions, come from ERA-40 for the period 1981 to 2002 and from ECMWF operational analyses from 2003 onwards. In addition, the initial atmospheric conditions are perturbed with unstable singular vectors and the ocean initial conditions are perturbed by adding sea surface temperature perturbations to the 5 member ensemble of ocean analyses. Stochastic perturbations to physical parameterization tendencies are active throughout the coupled forecast period. (Buizza et al. 1999)

S3 seasonal integrations are 7 months long (S2 integrations were only 6 months). Additionally, once per quarter an 11 member ensemble runs to 13 months, specifically designed to give an “ENSO outlook”. Back integrations have also been made to this range, once per quarter, with a 5 member ensemble.

The ocean analysis for System 3 extends back to 1959 and provides initial conditions for both real-time seasonal forecasts and the calibrating hindcasts. Although only the ocean analyses from 1981 onwards are used directly in S3, the earlier ocean analyses are used to analyse climate variability, and by the ENSEMBLES project for seasonal and decadal forecasts.

As for S2, the ocean data assimilation system for S3 is based on the optimum interpolation (OI) scheme developed for the HOPE model, but major upgrades have been introduced. In addition to subsurface temperature, the OI scheme now assimilates altimeter derived sea-level anomalies and salinity data. The system includes a multivariate bias-correction algorithm consisting of a prescribed a priori correction to temperature, salinity and pressure gradient, as well as a time-dependent bias term estimated on-line. The on-line bias correction is adaptive and allows for flow-dependent errors. In order to obtain a first-guess as input

to the OI analysis, it is necessary to force the ocean model with atmospheric fluxes. From January 1959 to June 2002 these are taken from ERA-40, and from the ECMWF operational NWP analysis thereafter.

Experiments show that data assimilation gives significant improvements in the mean state and variability of the upper ocean heat content, when compared to a wind forced ocean model run. Such improvements in the ocean initial conditions have a beneficial impact on the seasonal forecasts nearly everywhere, but especially in the west Pacific. A region where there is little impact is the equatorial Atlantic, probably because of significant model biases in this region. A fuller description of the ocean analysis system can be found in Balmaseda *et al.* (2006).

## 2.2. System 3 products

A set of real-time forecast products is released to the European and WMO Meteorological Services on the ECMWF website at 12Z on the 15<sup>th</sup> of each month, and a restricted set is available to the general public one week later (see the “seasonal forecast” section under [www.ecmwf.int/products/forecasts](http://www.ecmwf.int/products/forecasts)). The former set includes four categories of products, namely plumes for El Niño indices, horizontal maps of three-month anomaly statistics (ensemble mean and probabilities), “climagrams” (i.e. time series of indices representing area-averaged anomalies or pattern amplitudes) and tropical-storm indices. A fuller description of the new seasonal forecast products is available in Molteni *et al.* (2007).

In particular, information about rainfall forecasts over tropical regions can be obtained either from the spatial maps of ensemble-mean anomalies and probabilities of rainfall categories, or from the “climagrams” for area-averaged rainfall or rainfall-based monsoon indices. Among the spatial maps, the S3 products now include “tercile summary” plots which show, in a single map, probabilities of the most likely tercile category if (a) it is one of the outer categories (above upper tercile or below lower tercile) and (b) the probability of the category exceeds 40%. An example of this product, taken from the output of the forecast started on 1 May 2007, is shown in Fig. 1. The depicted probabilities are consistent with anomalies typical of La Nina conditions in the tropical Pacific and a positive phase of the Indian Ocean Dipole (e.g Saji *et al.* 1999).

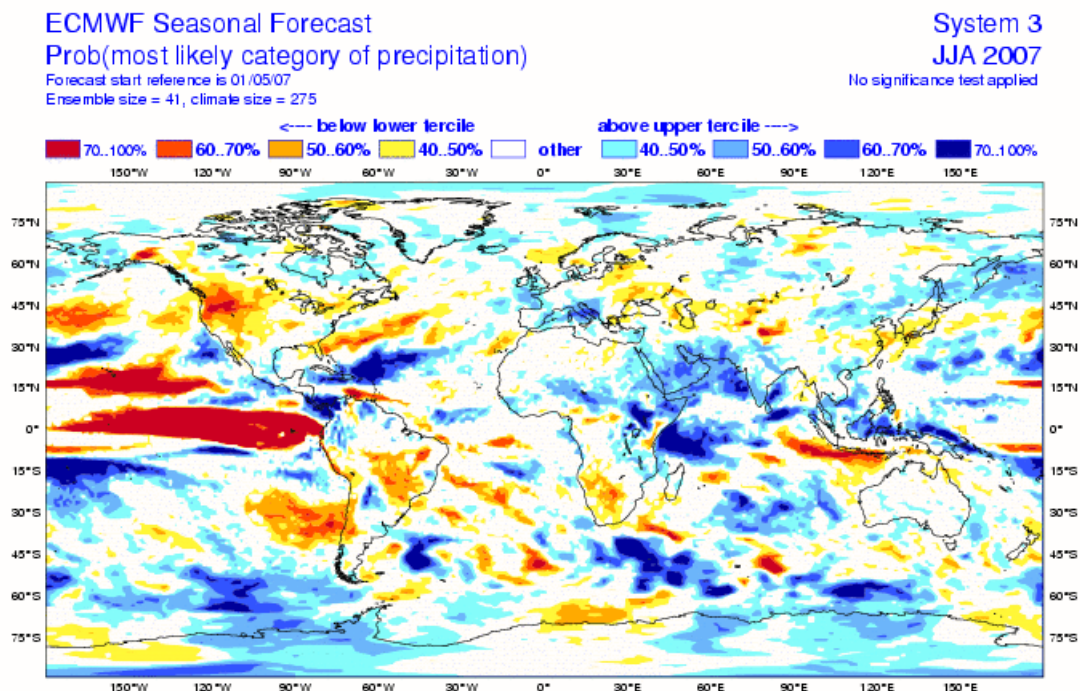


Figure 1: Tercile summary map for rainfall in JJA 2007 from the S3 seasonal forecast started on 1 May 2007. Shading indicates the probability of extreme tercile categories (either below lower tercile or above upper tercile) when such a probability exceeds 40%.

With regard to the “climagrams”, two kinds of rainfall time-series are displayed: averages over a set of 25 areas (shown in Fig. 2), or projections of forecast rainfall anomalies onto empirical orthogonal functions defined from observational data (namely, GPCP gridded data) over two monsoon-affected regions: west Africa and South Asia/tropical Indian Ocean. These indices of large-scale monsoon rainfall are complemented by an estimate of the ‘traditional’ All India Rainfall (AIR) index, which is obtained by averaging rainfall over the land points of the Indian peninsula with topographic height less than 1000 m. The patterns of the selected rainfall EOFs is shown in Fig 3 and the mask used for the AIR definition is displayed in Fig. 11.

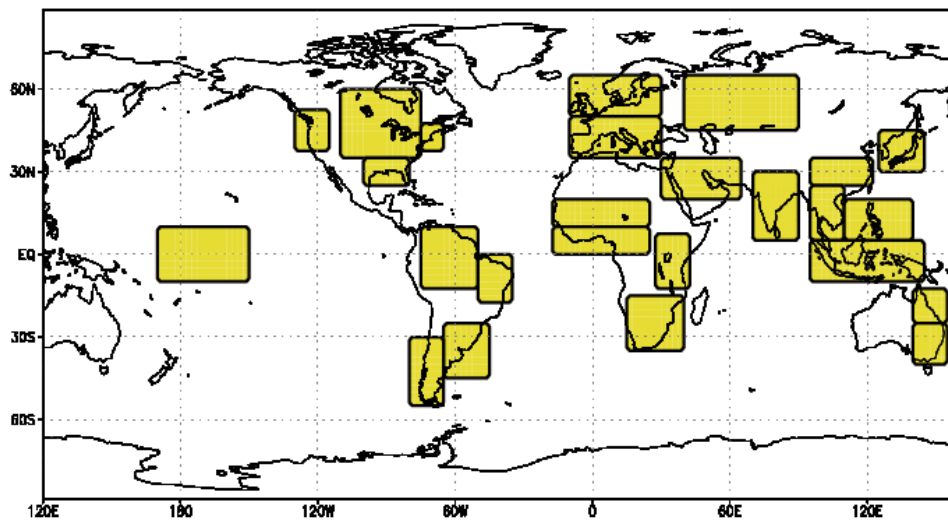


Figure 2: Areas used for the definition of regional monthly values of rainfall and 2m-temperature displayed in the “climagrams”

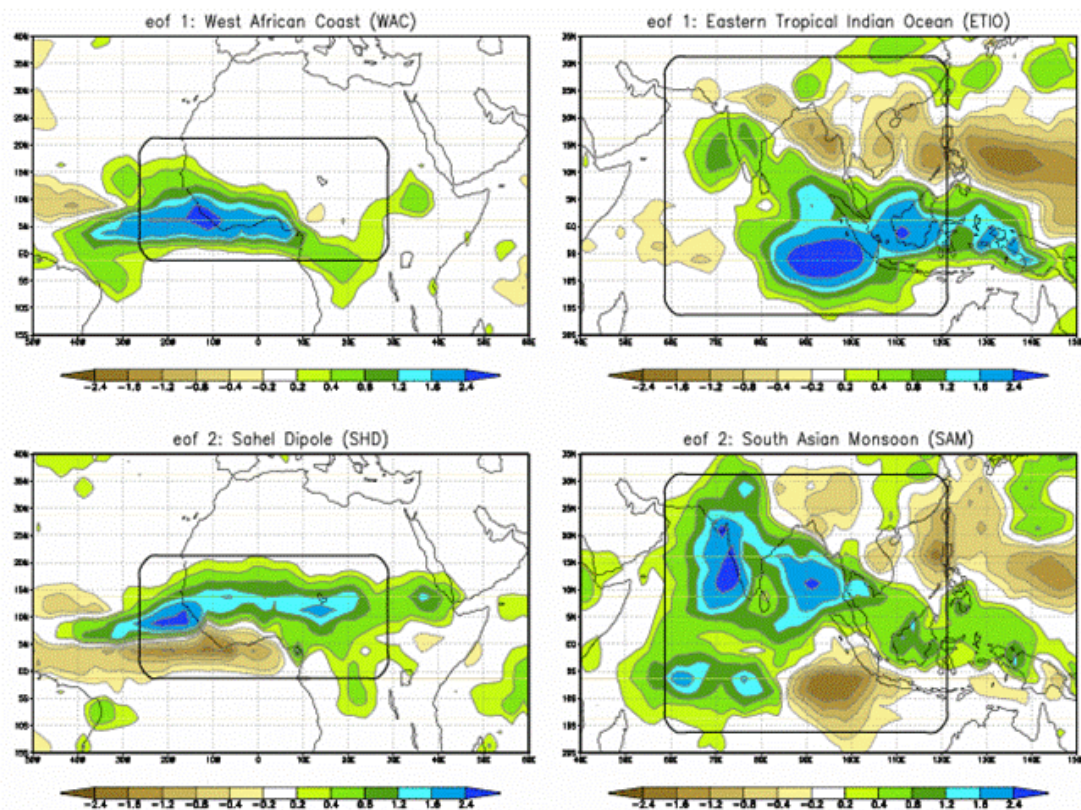


Figure 3: Left: first two EOF of west African monthly rainfall in the June-to-September season (EOF domain is shown by thick black line; data is from GPCP). Right: as left, but for a South Asia/Indian Ocean domain.

For a given index, and for each month in the seven-month forecast range, the climagram compares three distributions:

- the distribution derived from observational datasets (for rainfall, GPCP data) during the S3 hindcast period 1981–2005 (orange/yellow band);
- the distribution corresponding to the model climatology computed from the hindcast dataset (grey box/whiskers);
- the distribution from the 41-member ensemble forecast started at the beginning of the first month in the graph (purple box/whiskers).

For each distribution, the graph shows the median, the interval between the lower and upper terciles, and the interval between the 5th and 95th percentiles. As an example, the climagram for the AIR index from the 1 May 2007 forecast is shown in Fig. 4; the shift of the predicted distribution towards positive anomalies in the June-to-September period is again consistent with prevailing SST conditions in the tropical Pacific and Indian Ocean.

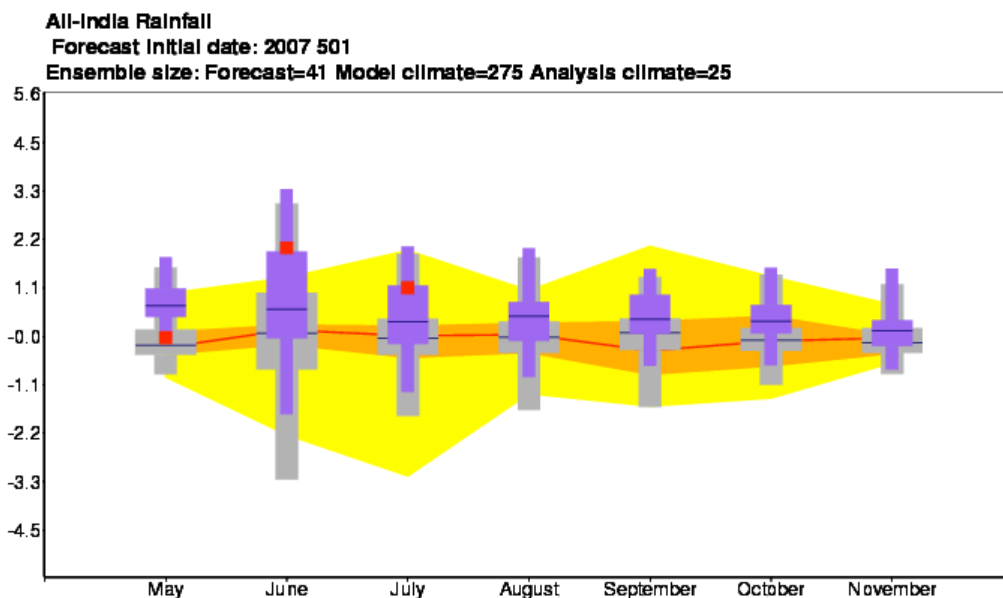


Figure 4: Climagram of All India Rainfall from the S3 seasonal forecast started on 1 May 2007. Distributions from observed climatology (orange/yellow band), model climatology (grey box/whiskers) and 41-member ensemble forecast (purple box/whiskers) are displayed. See main text for further explanation.

### 3. Potential and actual predictive skill for seasonal rainfall anomalies

Predicting rainfall anomalies is notoriously one of the most difficult tasks in extended range forecasting. Throughout the 1980's and early 1990's, the increased understanding of the role played by SST in shaping the distribution of tropical rainfall raised the prospect for skilful seasonal prediction for most tropical regions and for those mid-latitude regions most directly affected by tropical-extratropical interactions. This optimistic view was mainly based on the assumption of a quasi-linear superposition of SST-forced signals and internal atmospheric variability, acting on different time scales (e.g. Charney and Shukla 1981). Parallel to the growth of scientific understanding, the improvements in the ocean observing system for the tropical Pacific led to a much better specification of the ocean initial states for dynamical models of the coupled ocean-atmosphere system.

The fact that such advancements have not yet translated into a substantial increase in predictive skill over many tropical and extratropical regions is currently a reason for concern in the scientific community, and its

causes are a matter of debate (see the WCRP seasonal prediction position paper at [http://www.clivar.org/organization/wgsip/spw/spw\\_position.php](http://www.clivar.org/organization/wgsip/spw/spw_position.php)). One can point to the significant climate drift of most coupled GCMs, to the fact that inappropriate methodologies have been used in the past (see Wang et al. 2005), to the need of improving the ocean observing system over the tropical Atlantic and Indian oceans. These problems are likely to be alleviated in the near future by modelling and technological advances.

However, it should also be recognized that the dynamics of large-scale teleconnections and monsoon-like systems has substantial “internal” components which are either weekly dependent on SST, or interact with the SST-forced signal in a non-linear way. Indeed, not all tropical rainfall anomalies are associated with strong SST anomalies. Fig. 5 shows the rainfall anomalies over the tropical belt occurred during December 1997 and July 2002, two months characterized by heavy floods over East Africa and sever drought over India respectively. In Fig. 6, the SST anomalies in the same months are displayed. If the East African rainfall in Dec. 1997 can be reasonably attributed to the effect of the exceptional El Nino event and the warm SST anomalies over the western tropical Indian Ocean (e.g. Webster et al. 1999), it’s hard to find any strong SST signal which could justify the severity of the Indian drought in July 2002.

Therefore, in evaluating the skill of a seasonal prediction system, it is important to have a realistic estimate of the potential predictability limit, i.e. the upper limit in forecast skill purely induced by the dynamical amplification of initial errors in a perfect-model environment. With ensemble prediction systems, it is customary to assume that an upper limit for the skill of the ensemble mean can be estimated by verifying the ensemble-mean anomaly against the anomaly of each individual ensemble member, and then averaging the resulting score for all members. Such estimates should however be treated with caution, since they are

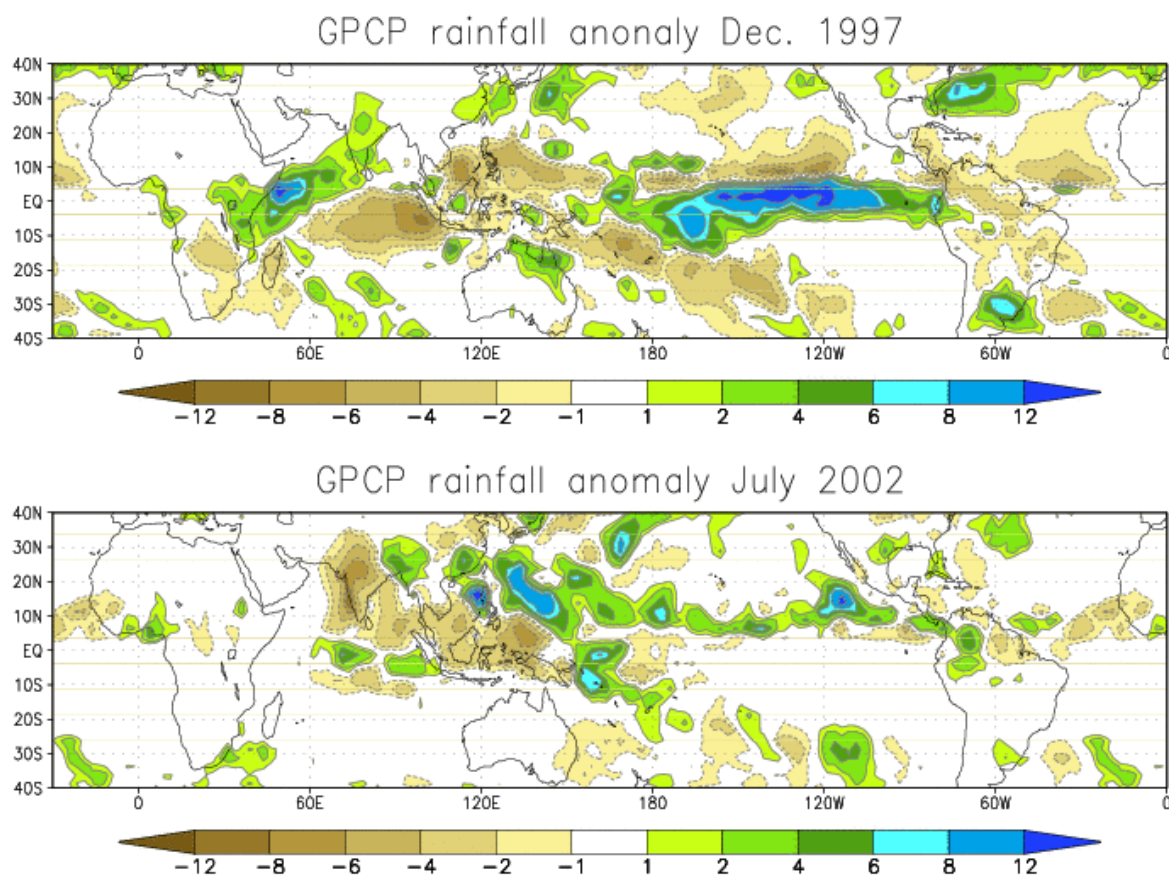


Figure 5: Rainfall anomalies in December 1997 and July 2002, from GPCP data (reference period: 1981-2005).

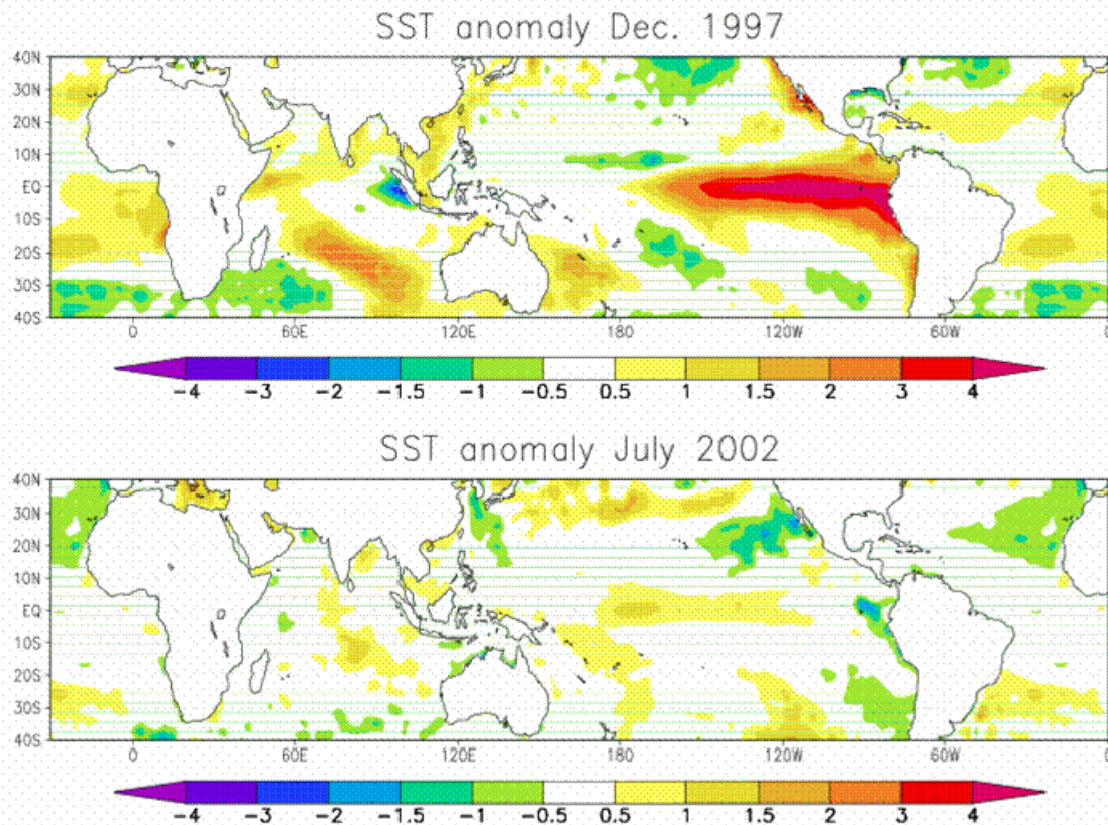


Figure 6: SST anomalies in December 1997 and July 2002, from ECMWF analysis data.

dependent on the level of internal variability generated by the coupled model, and on the amplitude of the ocean initial perturbations (contrarily to what happens in seasonal AGCM simulations, where atmospheric perturbations can be assumed to have grown to saturation after the first few weeks of integration).

Here, we first focus our attention on the predictability of 3-month-mean rainfall during the boreal winter and summer, averaged over the 25 regions selected for the production of “climagrams” (see Fig. 2). Specifically, we shall examine predictions for December-to-February (DJF) averages from ensemble hindcasts started on November 1st of each year in the 1981-2005 period, and for June-to-August (JJA) averages from ensembles started on May 1<sup>st</sup>. The correlation between ensemble-mean and verifying GPCP rainfall is displayed in the upper panels of Fig. 7 through the colour of the individual boxes (DJF on the left, JJA on the right). The bottom panels show, in the same graphical form, the upper-limit for such correlation estimated from the perfect-model assumption.

The following comments can be made on these results.

- In regions within or surrounding the tropical Pacific, which are directly affected by the ENSO phenomenon, the predictive skill is quite high, and in most cases only marginally lower than the potential predictability limit. The same is true for the Amazon Basin and southern Africa during the boreal winter.
- For extratropical regions, the actual predictive skill is generally much lower than the perfect-model estimates. Regions where such a difference is reduced appear to be southern Europe, north-west Asia and the La Plata basin during the respective summer seasons.
- The difference between potential and actual skill is also large in regions affected by monsoon systems during the boreal summer, namely West Africa, south and east Asia. In fact, the JJA predictions show almost no skill for regions on the northern and western side of the Indian Ocean.

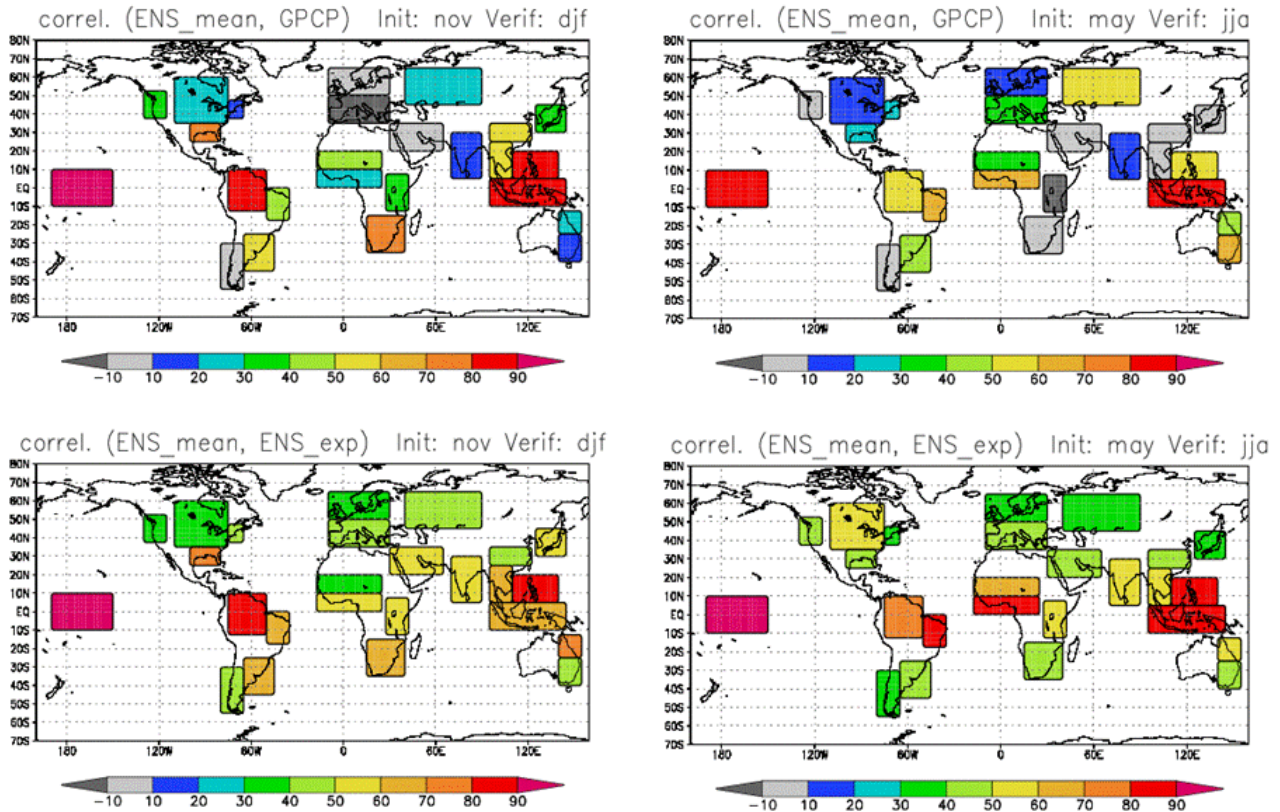


Figure 7: Top panels: Anomaly correlation between ensemble-mean rainfall and GPCP data, for DJF (left) and JJA (right). Hindcast ensembles are started on 1 November and 1 May respectively. Bottom panel: perfect-model predictability limit obtained by correlating ensemble-mean data with values from individual ensemble members.

The poor performance of system-3 on predicting JJA rainfall anomalies associated with the Asian monsoon problem is disappointing. One may wonder if this is mainly caused by errors in SST forecasts, an incorrect dynamical response to (actual) SST anomalies or to deficiencies in simulating continental rainfall even in the presence of a correct SST and large-scale flow. Fig. 8 shows a map of anomaly correlation between ensemble-mean and observed SST in the tropics, with estimates of 95% confidence levels derived by a bootstrap method. Although such correlations fall below the 95% significance level in the western equatorial

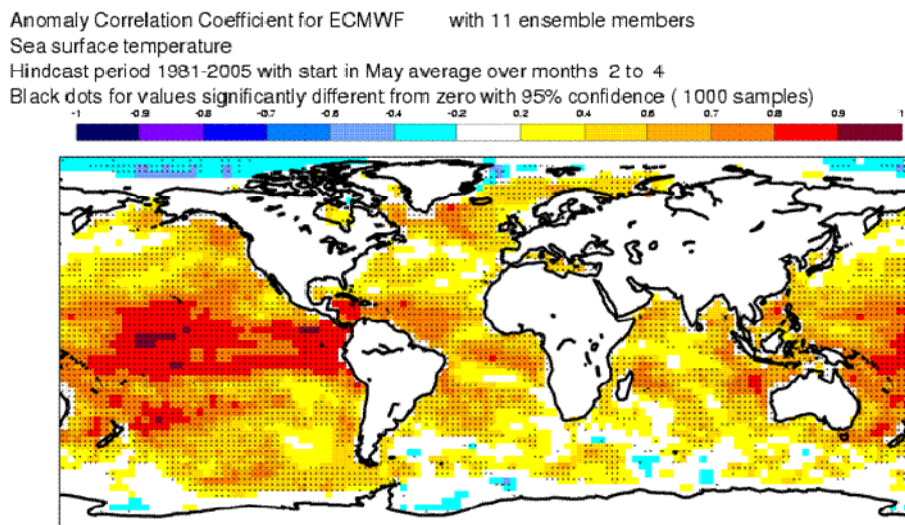


Figure 8: Anomaly correlation between ensemble-mean and observed SST anomalies in JJA, from ensembles started on 1 May.

Indian Ocean, the skill in the surrounding regions (and in southern tropical Atlantic) does not support the hypothesis that errors in predicted SST are the main culprit of the poor monsoon rainfall forecast. Rather, a comparison between observed and modeled standard deviations of monthly-mean rainfall reveals an excessive variability in model simulations over India at the beginning of the monsoon season. This can be deduced by the climagram for the AIR index shown in Fig. 4: the model rainfall variability in June (quantified by the extent of the grey box/whisker) appears to be at least twice as large as the observed variability (orange/yellow band). This problem is alleviated if July-to-September averages are considered (see below). Significant discrepancies between observed and modeled variability are also found over West Africa, with too strong variability close to the Atlantic coast and too little over Sahel (not shown).

If model deficiencies in simulating continental rainfall are indeed the main problem, we should expect System-3 to perform better in predicting rainfall indices representing the variability over larger tropical regions, including the ocean domains where the monsoon systems develop. The projections onto the regional rainfall EOFs shown in fig. 2b can be considered in this regard. Fig. 9 and 10 show time series of GPCP, ensemble-mean and individual ensemble member rainfall anomalies in JJA, projected onto two regional EOFs (referred to as the Eastern Tropical Indian Ocean pattern and the Sahel/Guinea Coast dipole respectively). The predictive skill of the ensemble mean indices is quite high, with 0.73 and 0.58 correlation respectively, and is close to the highest skill obtained for individual area-averages within the EOF domain. This raises the possibility of using regional EOFs to extrapolate the forecast information from ocean regions (where rainfall predictions are less affected by model errors) to the neighbouring continental regions.

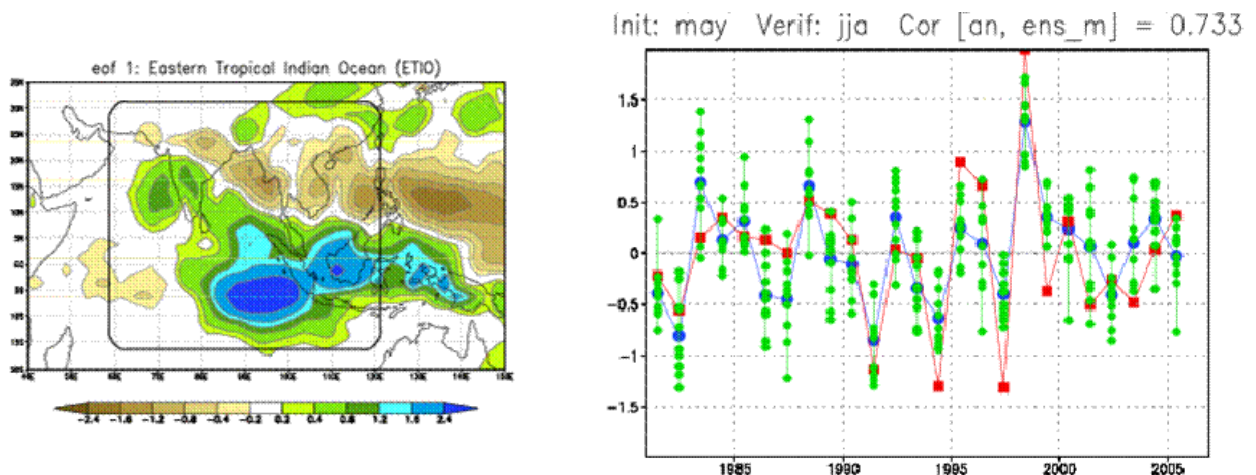


Figure 9: Left: First EOF of monthly rainfall (from GPCP data) in a South Asia/Indian Ocean domain (thick line). Right: projections of JJA mean rainfall anomalies on the EOF, for GPCP data (red squares), ensemble-mean hindcasts from 1 May (blue dots), individual ensemble members (green dots) in the 1981-2005 period.

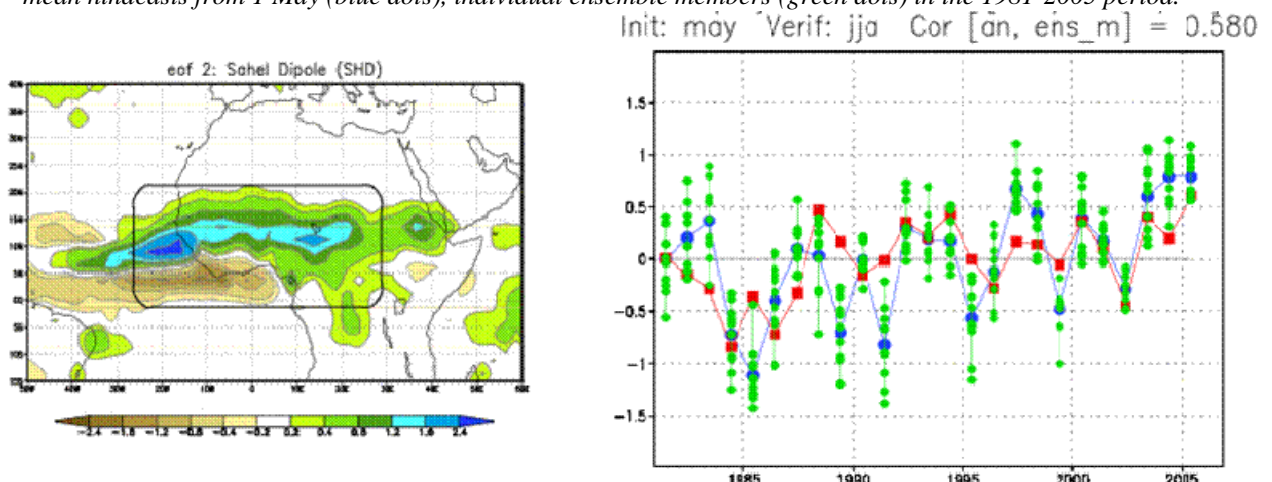


Figure 10: As in Fig. 9, but for the second rainfall EOF over West Africa and corresponding projections of JJA anomalies.

#### 4. Predictions of continental rainfall by EOF filtering: case studies for India and East Africa

In this section, a regional EOF approach to improve the forecast skill for continental rainfall will be evaluated in two specific cases: the All-India Rainfall (AIR) index during the boreal summer and the so-called ‘short rains’ over East Africa in boreal autumn.

The AIR index averaged over the whole summer monsoon season (June-to-September, JJAS) has often been used as a diagnostic parameter for the intensity of the Indian monsoon, or as a predictand in seasonal forecast systems (e.g. Rajeevan et al. 2004). Although it is widely accepted that the practical usefulness of such an index for societal application is limited, it remains a ‘first order’ indicator of the interannual variability of the summer monsoon over India. Therefore, a correct prediction the AIR index on seasonal time scale can be considered as a necessary (albeit non sufficient) condition for the delivery of useful seasonal forecasts over India.

As mentioned above, the AIR index is computed from System-3 output by averaging rainfall over all land grid-points in the 70-90E, 5-30N box (excluding Sri Lanka) whose elevation is less than 1000m (according to a grid-box-averaged topography). In Fig. 11, time series of observed and May-started hindcast values are plotted for averages over the full JJAS monsoon season and the JAS period only. The correlation between GPCP and ensemble-mean indices increases from 0.25 to 0.46 by excluding June data. Interestingly, June-only averages from the May hindcasts show a 0.35 correlation with observations, although their standard deviation is twice as large. Therefore, the fact that the correlation for the JJAS average is less than any weighted average of the June and JAS correlation is an indication of a *negative* correlation between the June and JAS predictions, and suggests that separate predictions for the onset and the mature phase of the monsoon may be more skilful than the traditional 4-month average.

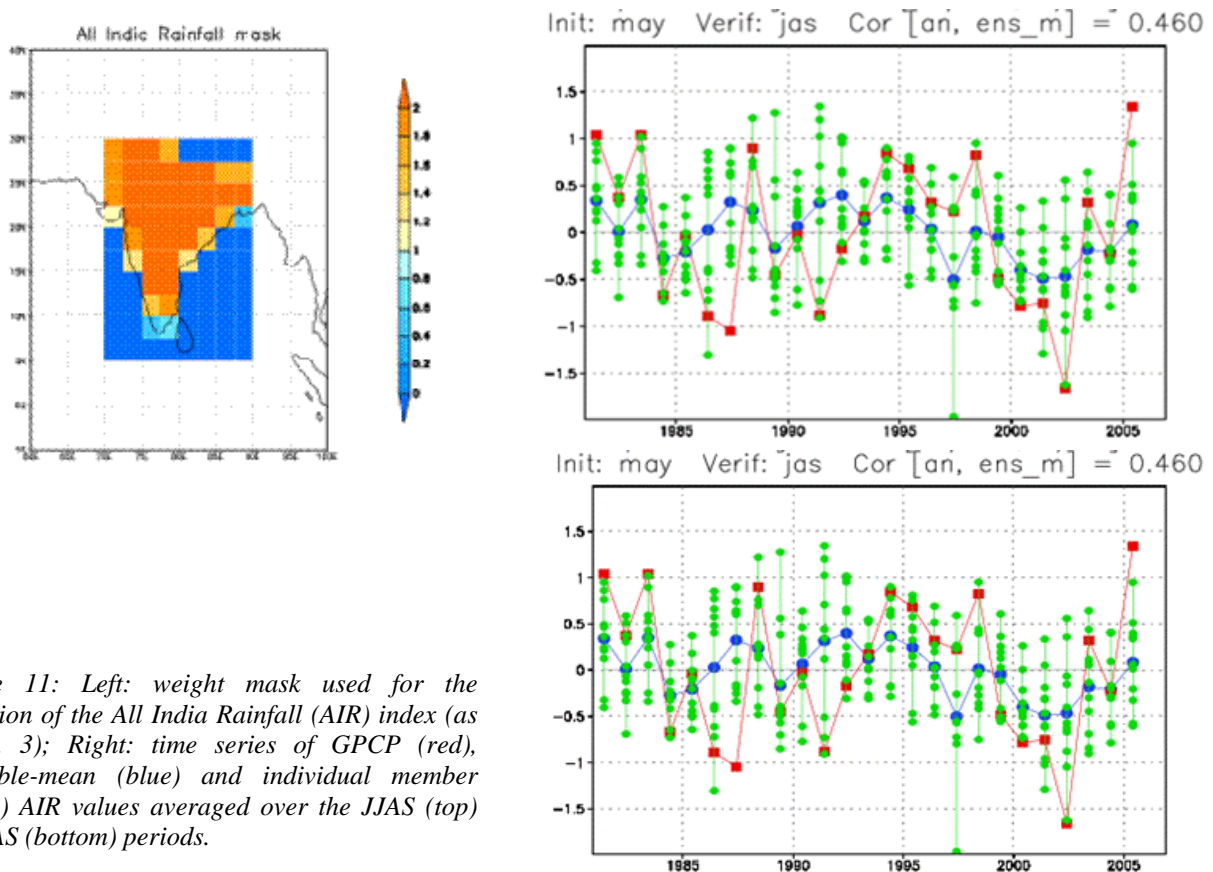


Figure 11: Left: weight mask used for the definition of the All India Rainfall (AIR) index (as in fig. 3); Right: time series of GPCP (red), ensemble-mean (blue) and individual member (green) AIR values averaged over the JJAS (top) and JAS (bottom) periods.

Concentrating on the JAS period, we now want to explore if we can further increase the skill of the forecast by a suitable spatial filtering of model data. To do so, we can proceed as follows:

- compute regional EOFs of *observed* monthly rainfall over a domain including the Indian subcontinent;
- project forecast data onto a suitable EOF subspace;
- construct EOF-filtered forecast fields by a linear combination of the selected EOFs and projection coefficients;
- average the filtered fields over the selected continental region, as previously done with ‘raw’ forecast data.

Note that computing the EOFs from observed, rather than modelled, data is not only needed to recover the ‘correct’ relationship between land and ocean values, but also avoids ‘over-tuning’ the procedure to a specific model and hindcast dataset.

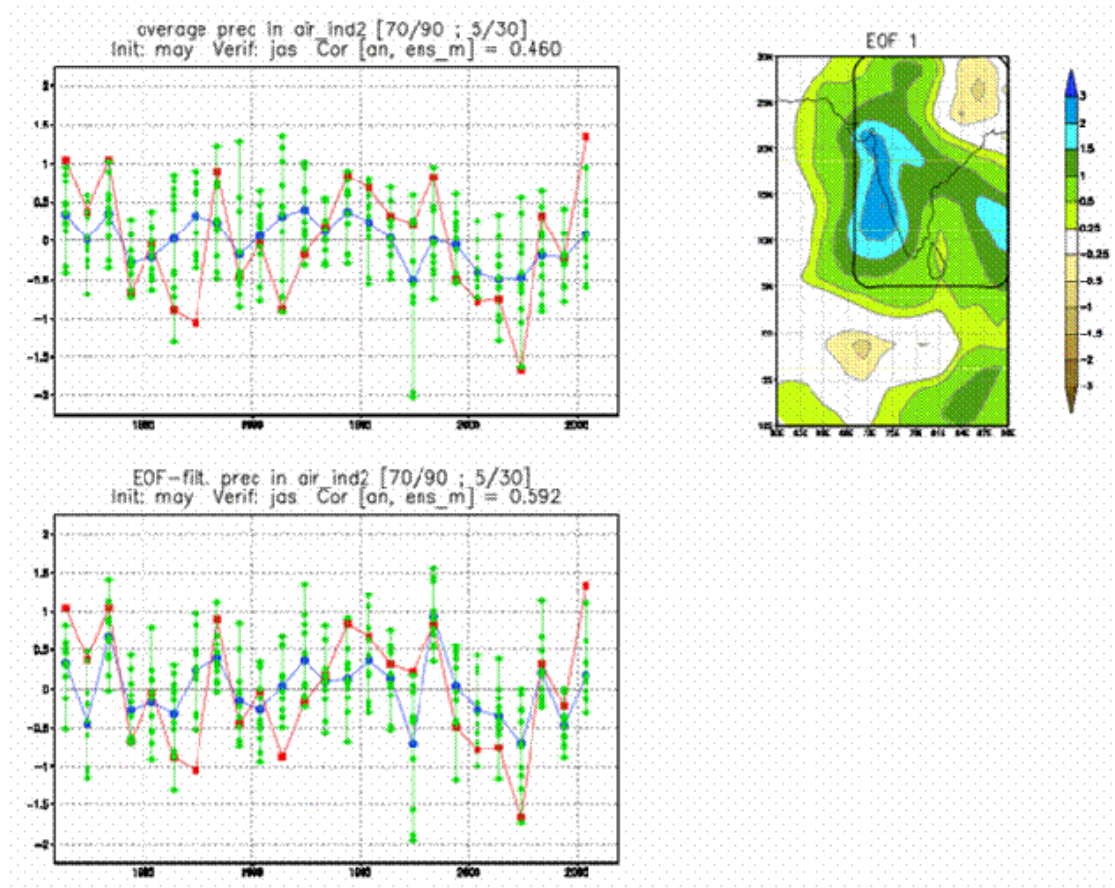


Figure 12: Time series of observed and model AIR data in the JAS season, from raw model data (top) and from model data filtered by projecting them onto the EOF shown in the right-hand panel. Colour coding as in Fig. 9.

A first test of this method for the AIR index was made using the first two EOFs of the wide South Asia-India Ocean domain shown in Fig. 3. In general, the larger the EOF domain with respect to the target area (India in this case), the higher is the number of EOFs needed to provide an effective reconstruction of the local data. In this case, the 2-EOF projection gave a correlation of 0.50 for JAS values, showing a positive but modest increase with respect to the original data result (0.46). However, it turned out that better results could be obtained with smaller EOF domains. The first EOF in the domain (55-90 E, 10S-30N), shown in the right-

top panel of Fig. 12, has a uniform sign over most of the Indian peninsula, but reproduces the well documented anti-correlation with north-east India and with the equatorial Indian Ocean. The projection of ensemble-mean values on this single EOF has a correlation of 0.59 with the AIR derived from GPCP data, increasing the explained variance by 65% with respect to the original forecasts. As noticeable from the time series plotted in Fig. 12, in the last 15 years of the hindcast record the filtered ensemble-mean value has the same sign as the GPCP values in all years except 1997, when a negative anomaly was predicted as a consequence of the strong El Niño event.

As a further test of the methodology, EOF filtering was applied to the prediction of the East African ‘short rains’ in the October-to-December (OND) season. Here, the target area is the East Africa box used in the System-3 “climagram” (see Fig. 2 and Fig. 7). As can be seen in the time series of GPCP and unfiltered hindcast data (top-left panel of Fig. 13), model-simulated data over land fail to reproduce the ENSO-IOD related variability visible in the GPCP record (see the maxima in OND 1982 and 1997), giving a near-zero correlation between ensemble-mean and GPCP data. However, the projection on the first EOF in a wider domain including East Africa and the western Indian Ocean is sufficient to recover a large part of the SST forced signal (see the agreement between observed and EOF-filtered interannual variations in the late 1990’s in the bottom panel of Fig. 13). EOF-filtering raises the anomaly correlation to a more acceptable value of 0.39, closer to a perfect-model estimate exceeding 0.5.

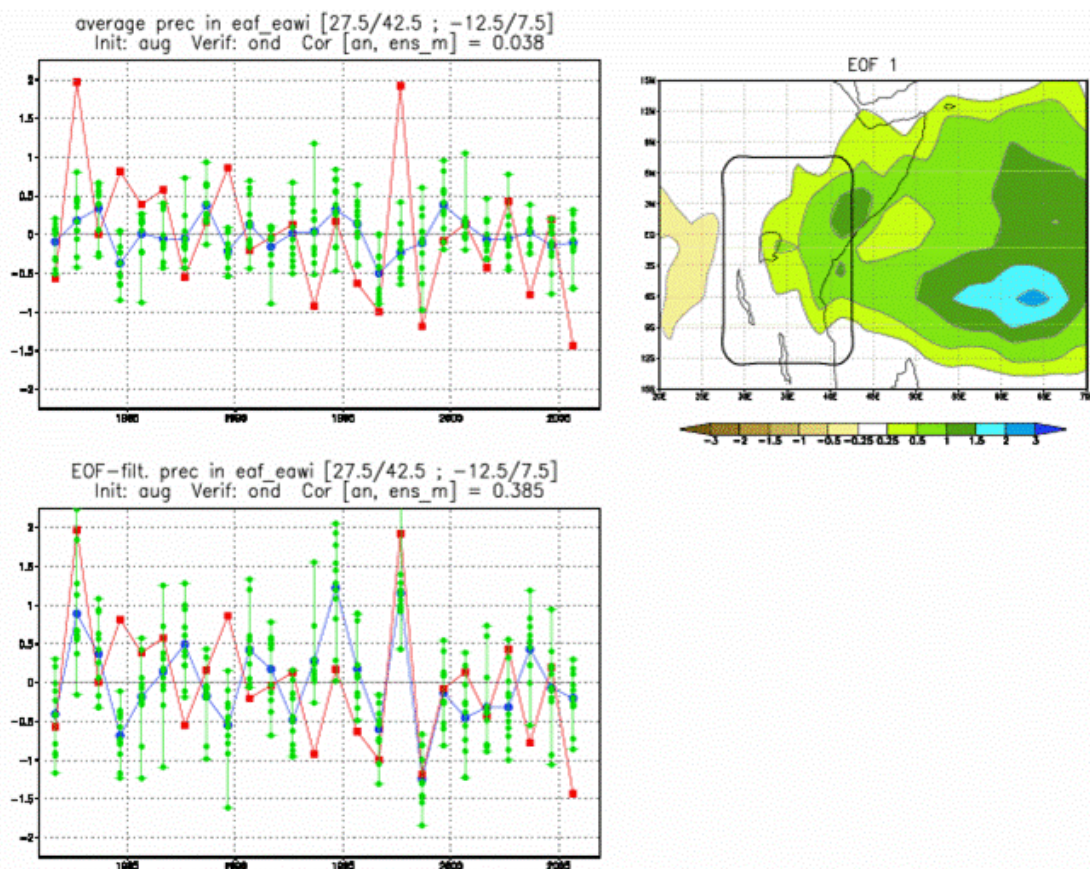


Figure 13: As in Fig. 12, but for raw and EOF-filtered rainfall anomalies averaged over east Africa in the OND season (the averaging area is shown by the thick line within the EOF pattern on the right).

The EOF-based correction method is, of course, only able to (partially) correct local model deficiencies, and offers a marginal improvement in regions where rainfall simulations are also affected by significant biases over the adjacent oceans. As a counter-example, EOF-filtered Sahel rainfall in summer shows no higher predictive skill than straight area-average forecasts. Still, by making use of observed teleconnection patterns,

the method appears to correct at least some of the most severe failures in tropical rainfall forecasts from System-3, giving a fairer assessment of the potential value of predictions by coupled GCMs.

## 5. Predictions of June rainfall over India with the VarEPS-Monthly system

June is the month during which monsoon onset occurs over the Indian peninsula. Although the definition of a precise onset date is probably a rather abstract exercise, it is clear that capturing the approximate time of the transition from a dry to a wet regime is important for a skillful prediction of June rainfall over India. In the previous section, we showed that System-3 hindcast ensembles started on the 1<sup>st</sup> of May have a modest skill as far as the June AIR is concerned, and are affected by a strong overestimation of interannual variability. In this section, we investigate whether using a prediction model with higher horizontal resolution and a starting date closer to the beginning of June brings any improvement to the AIR forecast during the early phase of the monsoon.

ECMWF has been running a monthly ensemble forecast system since 2002, using the same coupled model used for seasonal forecast, but with a greater number of ensemble members and (until the introduction of System-3 in March 2007) with higher horizontal resolution in the atmospheric component (see Vitart 2002). From March 2008, the medium-range variable-resolution Ensemble Prediction System (VAREPS; Buizza et al. 2007) and the monthly forecast system have been merged into a single ensemble system, which runs up to 15 days every day and up to 32 days once a week. In the first 10 days of integration, the ECMWF atmospheric model is run with a spectral truncation of T399 and an equivalent horizontal resolution of about 50 km, while the ocean model is forced with the momentum, heat and freshwater fluxes computed by the atmospheric model. After day 10, the atmospheric and ocean components are fully coupled, and the atmospheric resolution is reduced to about 80 km (T255).

Although in its first operational implementation the VAREPS-monthly system will be integrated for a maximum of 32 days, we have tested the system in a set of 45-day experiments started on the 15<sup>th</sup> of May of each year from 1991 to 2007. The May 15<sup>th</sup> initial date has been chosen to coincide with the actual release of the seasonal forecast with May 1<sup>st</sup> initial condition. Since the monthly forecast is released in near-real time, one can compare June forecasts from two systems which are (potentially) available to users within 24 hours from each other.

The time series of ensemble-mean AIR for June, the ensemble spread and the verifying GPCP data are plotted in Fig. 14. The correlation between ensemble-mean and GPCP values in the 1991-2005 period is 0.62, much higher than the 0.29 value obtained from the System-3 hindcasts for the same years started on 1 May (and even higher than the 0.50 correlation obtained from seasonal hindcasts started on 1 June). In addition, the VAREPS-monthly predictions appear to suffer less from the problem of excessive interannual variability detected in System-3 data (note that the atmospheric model cycles used in the two sets of experiments are nearly identical from the physical point of view).

If an improvement in the predictive skill for monthly totals was somehow expected, a more challenging test is given by the verification of 5-day-mean (pentad) values at the beginning of June, when monsoon rains usually start affecting southern India. Time series for the 1-5 June and 6-10 June pentads, which correspond to forecast days 16-20 and 21-25 respectively, are shown in Fig. 15, using ERA-40 estimates (integrated by operational products after 2001) for verification. The correlation of ensemble-mean and re-analysis AIR data is 0.79 for the 16-to-20-day forecasts and 0.76 for the 21-to-25-day forecast. Even taking into account the greater consistency of re-analysis and forecast data (obtained, however, with very different model cycles and horizontal resolution), the level of achieved skill is remarkable. It shows that the VAREPS-monthly system is capable to deliver useful information on Indian rainfall during a critical transition period, and provide a valid complement to the seasonal predictions for the mature phase of the monsoon.

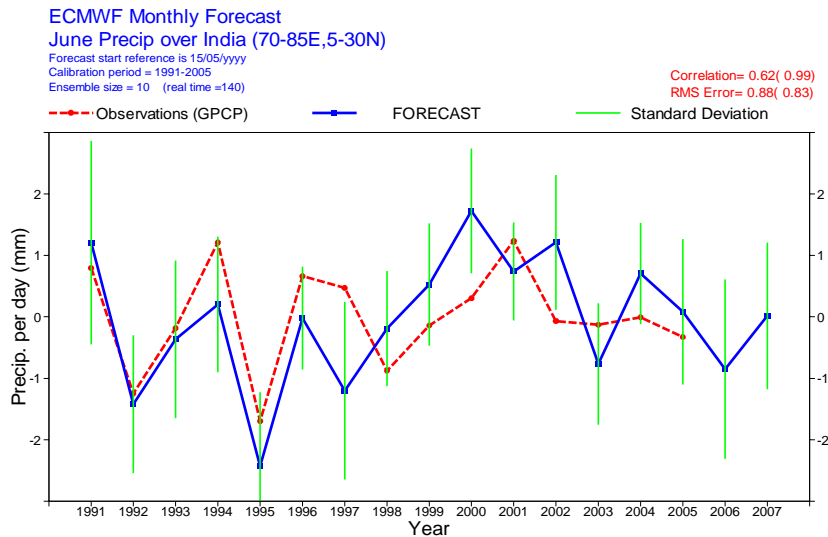


Figure 14: Time series of June AIR values from 45-day experiments with the VAREPS-monthly forecast system started on 15 May 1991 to 2007. Blue line: ensemble mean, green bar: range within 1 standard deviation from the mean, red line: GPCP data.

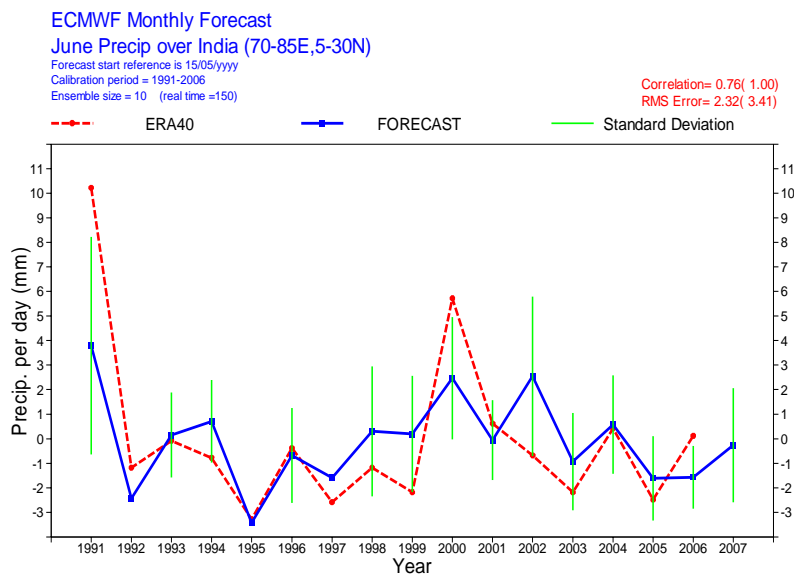
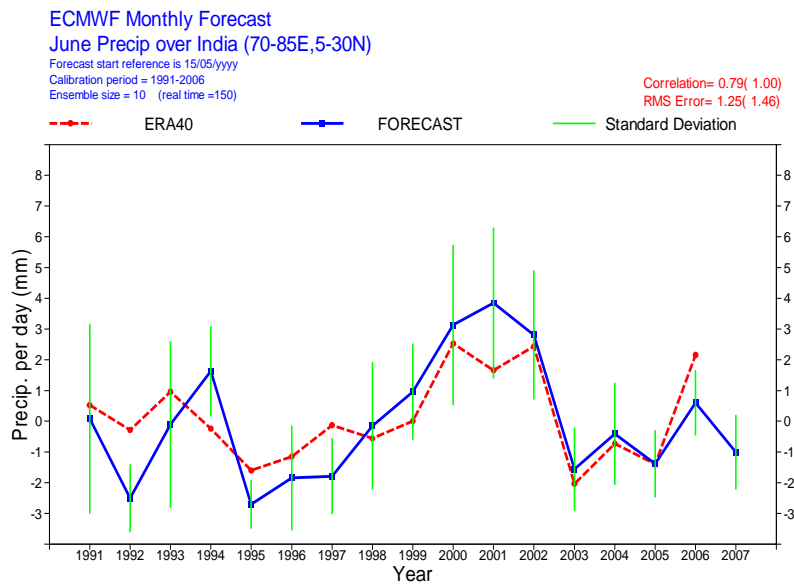


Figure 15: As in Fig. 14, but for predicted and observed rainfall anomalies in the 1-5 June pentad (fc. day 16-20) (top), and in the 6-10 June pentad (fc. day 21-25) (bottom).

## 6. Conclusions

In the last 12 months, ECMWF has implemented new systems for both its seasonal and monthly forecasts. The main purpose of this paper was to assess the potentiality of such systems with regard to prediction of rainfall anomalies in tropical regions, with particular attention to south Asian monsoon rainfall, and to present simple post-processing techniques to partially correct local model biases.

An assessment of actual predictive skill and potential (i.e. perfect model) predictability of 3-month-mean rainfall averaged over specific regions, obtained from diagnosing the System-3 seasonal hindcast ensembles, led to the following conclusions:

- In regions within or surrounding the tropical Pacific, which are directly affected by the ENSO phenomenon, the predictive skill is quite high, and in most cases only marginally lower than the potential predictability limit. The same is true for the Amazon Basin and southern Africa during the boreal winter.
- For extratropical regions, the actual predictive skill is generally much lower than the perfect-model estimates. Regions where such a difference is reduced appear to be southern Europe, north-west Asia and the La Plata basin during the respective summer seasons.
- The difference between potential and actual skill is also large in regions affected by monsoon systems during the boreal summer, namely west Africa, south and east Asia.

It was also shown that, when projections on regional EOF patterns are used as predictands, the predictive skill for such rainfall indices is usually close to the highest skill obtained for individual area-averages within the EOF domain. This raises the possibility of using regional EOFs to extrapolate the forecast information from ocean regions (where rainfall predictions are less affected by model errors) to the neighbouring continental regions. It was shown that EOF filtering can significantly improve the predictive skill for all-India rainfall in the mature phase of the monsoon (July-to-September) and for the East-African ‘short rains’ in October-to-December. (Forecast skill for Sahel summer rainfall, on the other hand, was hardly improved by this technique).

Finally, it was shown that separate predictions for the onset and mature phase of the Indian monsoon should be considered rather than the traditional 4-month (JJAS) averages. While the seasonal forecast System 3 provides useful predictive information for the latter period (especially when EOF filtering is applied), predictions for the early June phase were much better handled by the higher-resolution VAREPS-monthly system, which is run in nearly-real time. Not only were June totals better predicted, but significant skill was obtained for individual pentad periods at the beginning of June, despite a forecast lead time going from 16 to 25 days. Further experimentation (not discussed above) indicate that, as far as Indian summer rainfall is concerned, the advantage of the monthly system over its seasonal counterpart is indeed largest at the beginning of the monsoon season.

The results discussed above, while pointing to the need for further progress on modelling and initialization, indicate that useful predictive information can be extracted from dynamical ensemble predictions of tropical rainfall, by combining the strength of different systems and employing post-processing techniques to correct local model biases. It is also evident that reliable estimates of potential predictability are needed for a proper assessment of forecast skill, in order to direct further modelling effort towards those areas and phenomena where model deficiencies are still the main limiting factor to actual forecast quality.

*Acknowledgements*

The development of the ECMWF seasonal and monthly prediction systems is a collective effort which has involved many scientists in the Research and Operations Departments. In particular, we wish to gratefully acknowledge the contributions of current and former colleagues D. Anderson, R. Buizza, K. Mogensen, F. Doblas-Reyes, T. Palmer, A. Vidard and A. Weisheimer in the Probabilistic Forecasting and Diagnostic Division of ECMWF.

**7. References**

- Anderson D., T. Stockdale, M. Balmaseda, L. Ferranti, F. Vitart, F. Molteni, F. Doblas-Reyes, K. Mogensen and A. Vidard, 2006: Seasonal Forecasting System 3. *ECMWF Technical Memo* No 503. Available from [www.ecmwf.int](http://www.ecmwf.int) .
- Balmaseda, M., A. Vidard and D. Anderson, 2006: The ECMWF System 3 ocean analysis system. *ECMWF Technical Memo* No 508. Available from [www.ecmwf.int](http://www.ecmwf.int) .
- Buizza, R., Miller, M., & Palmer, T. N., 1999: Stochastic representation of model uncertainties in the ECMWF Ensemble Prediction System. *Q. J. R. Meteorol. Soc.*, **125**, 2887-2908.
- Buizza, R., J-R. Bidlot, N. Wedi, M. Fuentes, M. Hamrud, G. Holt, and F. Vitart, 2007: The new ECMWF VAREPS (Variable Resolution Ensemble Prediction System). *Q. J. R. Meteorol. Soc.*, **133**, 681-695.
- Charney, J. G., and J. Shukla, 1981: Predictability of monsoons. In: *Monsoon Dynamics*, Eds: J. Lighthill and R. P. Pearce, Cambridge University Press, pp. 99-109
- Gadgil, S., M. Rajeevan, and R. Nanjundiah, 2005: Monsoon prediction - Why yet another failure? *Current Science*, **88**, 1389-1400.
- Molteni, F., L. Ferranti, M. Balmaseda, T. Stockdale and F. Vitart, 2007: New web products for the ECMWF seasonal forecast System-3. *ECMWF Newsletter* No. 111, 28-33. Available from [www.ecmwf.int](http://www.ecmwf.int) .
- Rajeevan, M., D.S. Pai, S.K. Dikshit and R.R. Kelkar, 2004: IMD's New Operational Models for Long Range Forecast of South-west Monsoon Rainfall over India and their verification for 2003. *Current Science*, **86**, 422-431.
- Saji, N. H., B. N. Goswami, P. N. Vinayachandran and T. Yamagata, 1999: A dipole mode in the tropical Indian Ocean, *Nature*, **401**, 360-363.
- Wang B., Q. Ding, X. Fu, I.-S. Kang, K. Jin, J. Shukla and F.J. Doblas-Reyes (2005). Fundamental challenge in simulation and prediction of summer monsoon rainfall. *Geophysical Res. Letters*, **32**, L15711, doi:10.1029/2005GL022734.
- Webster, P. J., T. Hopson, C. Hoyos, A. Subbiah, H.- R. Chang, R. Grossman, 2006: A three-tier overlapping prediction scheme: Tools for strategic and tactical decisions in the developing world. In *Predictability of Weather and Climate*, Ed. T. N. Palmer, Cambridge University Press. pp. 645-673.
- Webster, P. J., A. Moore, J. Loschnigg and M. Leban: 1999: Coupled ocean-atmosphere dynamics in the Indian Ocean during 1997-98. *Nature*, **401**, 356-360
- Xavier P.K., Goswami B. N., 2007: A promising alternative to prediction of seasonal mean all India rainfall, *Current Science*, **93**, 195-202.